Bioconjugate Chemistry

Article

pubs.acs.org/bc

Synthesis and in Vitro and in Vivo Evaluation of SiFA-Tagged Bombesin and RGD Peptides as Tumor Imaging Probes for Positron Emission Tomography

Simon Lindner,*[,†] Christina Michler,[†] Stephanie Leidner,[†] Christian Rensch,[‡] Carmen Wängler,[†,§] Ralf Schirrmacher,[∥] Peter Bartenstein,[†] and Björn Wängler*[,⊥]

[†]Department of Nuclear Medicine, University Hospital Munich, Ludwig-Maximilians-University, 81377 Munich, Germany

[‡]GE Global Research, 85748 Garching, Germany

[§]Biomedical Chemistry, Department of Clinical Radiology and Nuclear Medicine and [⊥]Molecular Imaging and Radiochemistry, Department of Clinical Radiology and Nuclear Medicine, Medical Faculty Mannheim of Heidelberg University, 68167 Mannheim, Germany

[∥]McConnell Brain Imaging Centre, Montreal Neurological Institute, McGill University, Montreal, Quebec H3A 2B4, Canada

Supporting Information

ABSTRACT: Gastrin-releasing-peptide (GRP)-receptors and $\alpha_v\beta_3$-integrins are widely discussed as potential target structures for oncological imaging with positron emission tomography (PET). Favored by the overexpression of receptors on the surface of tumor cells good imaging characteristics can be achieved with highly specific radiolabeled receptor ligands. PEGylated bombesin (PESIN) derivatives as specific GRP receptor ligands and RGD (one-letter codes for arginine-glycine-aspartic acid) peptides as specific $\alpha_v\beta_3$ binders were synthesized and tagged with a silicon-fluorine-acceptor (SiFA) moiety. The SiFA synthon allows for a fast and highly efficient isotopic exchange reaction at room temperature giving the [^{18}F]fluoride labeled peptides in up to 62% radiochemical yields (d.c.) and ≥99% radiochemical purity in a total synthesis time of less than 20 min. Using nanomolar quantities of precursor high specific activities of up to 60 GBq μmol^{-1} were obtained. To compensate the high lipophilicity of the SiFA moiety various hydrophilic structure modifications were introduced leading to significantly reduced logD values. Competitive displacement experiments with the PESIN derivatives showed a 32 to 6 nM affinity to the GRP receptor on PC3 cells, and with the RGD peptides a 7 to 3 μM affinity to the $\alpha_v\beta_3$ integrins on U87MG cells. All derivatives proved to be stable in human plasma over at least 120 min. Small animal PET measurements and biodistribution studies revealed an enhanced and specific accumulation of the RGD peptide ^{18}F-SiFA-LysMe$_3$-γ-carboxy-D-Glu-RGD (**17**) in the tumor tissue of U87MG tumor-bearing mice of 5.3% ID/g whereas the PESIN derivatives showed a high liver uptake and only a low accumulation in the tumor tissue of PC3 xenografts. Stability studies with compound **17** provided further information on its metabolism in vivo. These results altogether demonstrate that the reduction of the overall lipophilicity of SiFA tagged RGD peptides is a promising approach for the generation of novel potent ^{18}F-labeled imaging agents.

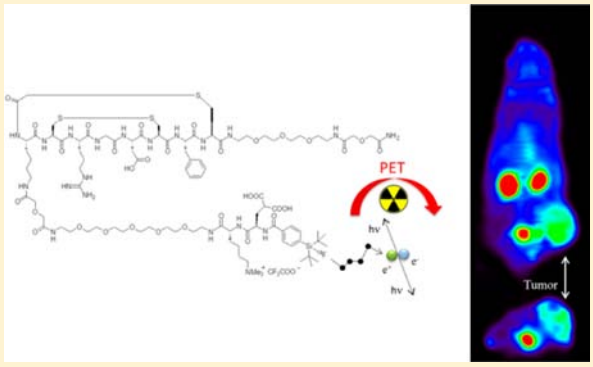

INTRODUCTION

The silicon-fluorine-acceptor (SiFA) methodology is a versatile approach for the radiolabeling of a broad range of compounds with the positron emitting radionuclide fluorine-18 (^{18}F). It has been applied to small molecules, even though best results were obtained with peptides and proteins.[1,2] Its great advantages are a fast and highly efficient isotopic exchange reaction, very mild reaction conditions, an easy purification procedure requiring no HPLC (high performance liquid chromatography), and high specific activities of the radiolabeled products. However, despite all beneficial properties, SiFA containing radiotracers have often revealed a high lipophilicity which was shown to entail poor in vivo characteristics and therefore limits their application for diagnostic imaging purposes in the clinic.[3] Some efforts have been undertaken recently to overcome this problem with modified silicon-containing building blocks.[4,5] Another possibility is the introduction of polar auxiliaries into the structure to compensate the high lipophilicity in favor of an improved pharmacokinetic profile of the radiotracer.

We intended to investigate this approach on bombesin and RGD (one-letter codes for arginine-glycine-aspartic acid) analogues. Bombesin peptides are ligands of the gastrin-

Received: January 7, 2014
Revised: March 24, 2014
Published: March 25, 2014

dx.doi.org/10.1021/bc400588e | *Bioconjugate Chem.* 2014, 25, 738−749

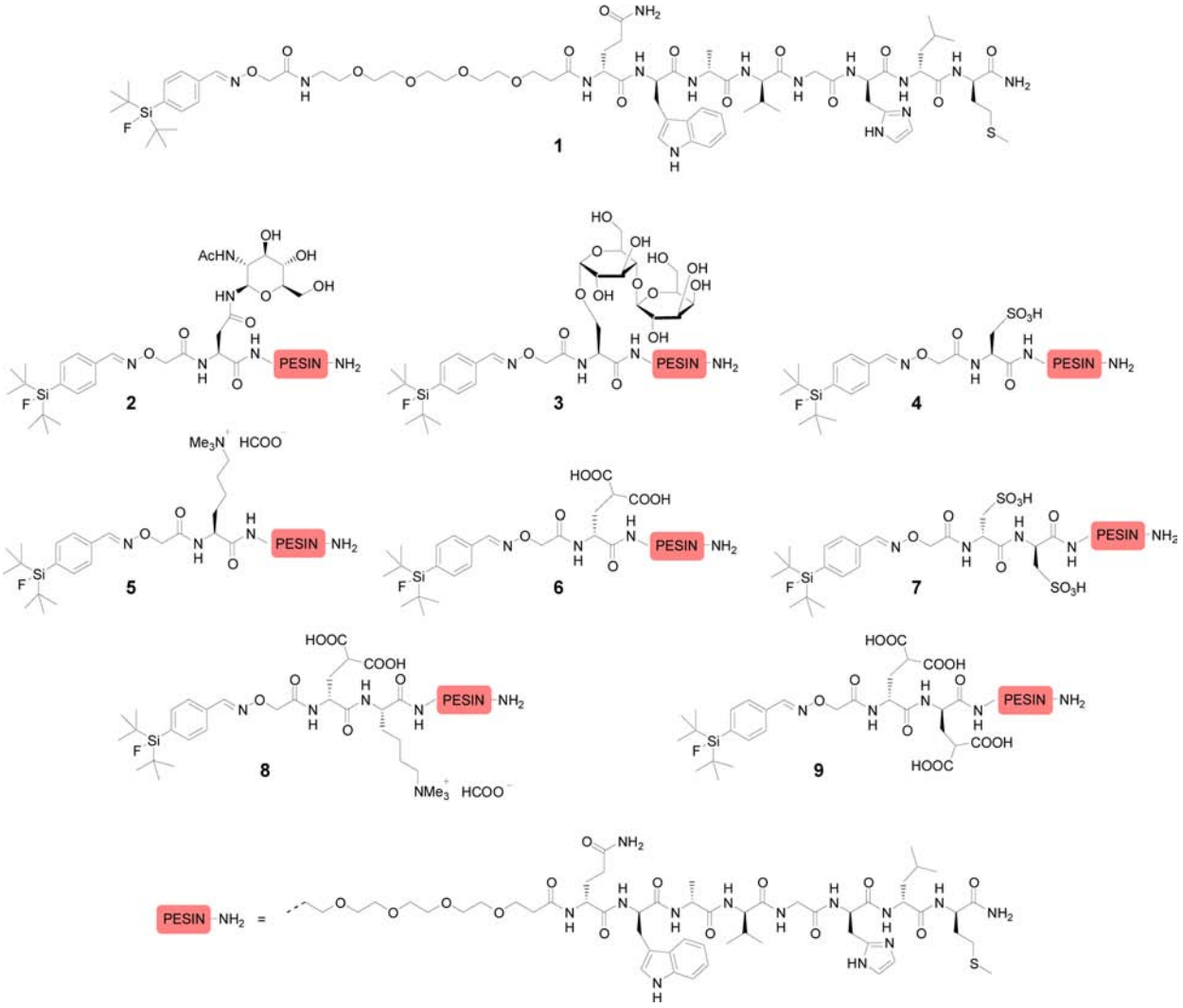

Figure 1. Structures of SiFA-PESIN (**1**) and SiFA-PESIN derivatives **2**−**9**.

releasing-peptide (GRP)-receptor which is overexpressed on several tumor tissues such as prostate, breast, ovarian, lung, colon, and gastrinoma cancers.[6,7] For that reason, GRP receptors are a favorable target structure for tumor visualization with imaging techniques such as PET (positron emission tomography). Many different bombesin derivatives have been developed so far,[8−16] but most suffer from poor pharmacokinetic properties. The most promising peptide is PESIN (PEGylated bombesin), as it exhibits favorable characteristics such as high stability in vivo and good tumor uptake.[17,18] The structure of PESIN is derived from the natural GRP-receptor ligands gastrin-releasing-peptide and bombesin sharing the same C-terminal region of 7 amino acids. This truncated peptide sequence is the pharmacophore and responsible for receptor binding. A PEG_4 motif is inherently present in the molecule which serves as hydrophilic spacer separating the pharmacophore from remaining structural motifs and the labeling moiety.

Similar experiments were envisaged with RGD peptides, an additional class of important bioactive molecules with high affinity to $\alpha_v\beta_3/\alpha_v\beta_5$ integrins for the imaging of angiogenesis.[19,20] Integrins are cell adhesion receptors which are upregulated in the new blood vessels of growing tumors providing the ability to monitor tumor growth and metastasis. RGD peptide ^{18}F-AH111585, nowadays named [^{18}F]-fluciclatide, exhibited good preclinical results and was successfully translated into human studies which encouraged us to combine its peptidic scaffold with the SiFA chemistry and to further investigate its in vitro and in vivo properties.[21−28]

Herein, we report on the synthesis and radiolabeling of SiFA tagged PESIN and RGD peptides. Hydrophilic auxiliaries were inserted in favor of improved pharmacokinetics. In vitro and in vivo experiments were carried out to evaluate whether this approach is feasible.

RESULTS

We intended to design a series of new SiFA-tagged PESIN derivatives with a variety of hydrophilic auxiliary amino acids embedded into the peptide backbone (Figure 1). Starting from uncharged sugar based residues such as glucose and lactose derived amino acids, we focused on carboxylic acid and sulfonic acid functionalities which are negatively charged under physiological conditions. Furthermore, positively charged quaternary ammonium groups and combinations thereof were considered in the design and synthesis of the peptides.

Synthesis and Radiochemistry. The PESIN scaffold was constructed via solid-phase peptide synthesis using the standard Fmoc strategy (Scheme 1). The polar auxiliary (Aux) and a

dx.doi.org/10.1021/bc400588e | Bioconjugate Chem. 2014, 25, 738−749

Scheme 1. Synthesis of [^{18}F]SiFA-Labeled PESIN Derivatives

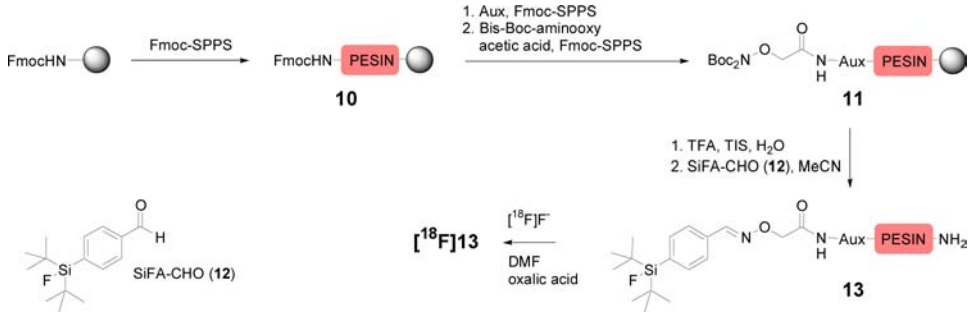

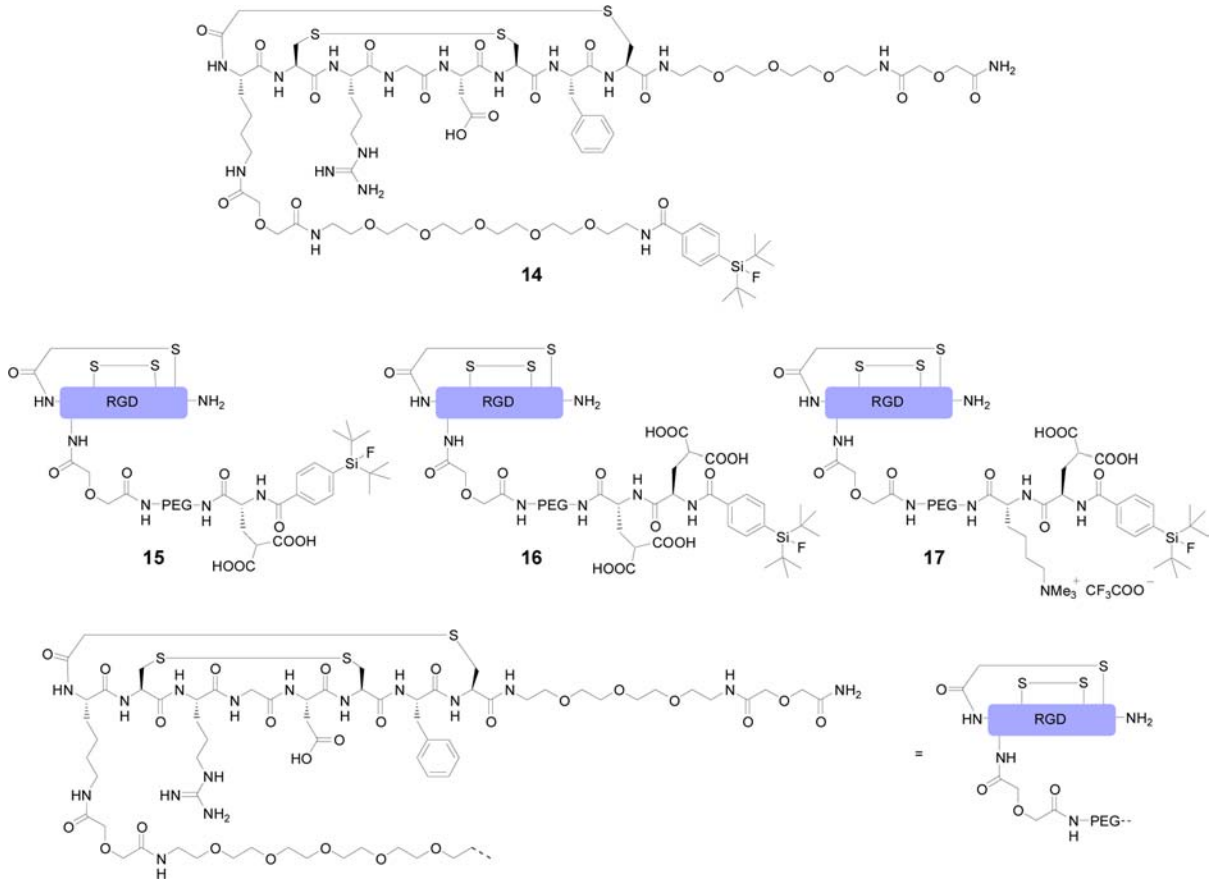

Figure 2. Structures of SiFA-RGD (**14**) and SiFA-RGD derivatives **15**−**17**.

terminal bis-Boc-aminooxyacetic acid were attached on solid support. After cleavage of the peptide from the resin, SiFA-CHO (**12**) was coupled to the aminooxyacetic acid functionalized peptide in the liquid phase via oxime formation to yield the labeling precursor **13**. The synthesis of SiFA-CHO (**12**) was described earlier.[29]

Amino acids which reduced the lipophilicity of PESIN derivatives most effectively were chosen for the generation of novel RGD peptides (Figure 2). Among them, carboxylic acid and ammonium based residues proved to be most appropriate for the implementation into the complex synthesis approach.

RGD peptides were also synthesized on solid support via Fmoc based solid phase peptide synthesis (Scheme 2). The thioether bridge was formed by condensation of an acetic acid functionalized thiol residue with the deprotected N-terminus. Thallium trifluoroacetic acid yielded the disulfide by deprotection of both remaining thiols and concomitant oxidative coupling. The side chain of a Lysin amino acid was connected to PEGylated linker **21** which enabled the direct attachment of polar amino acids (Aux) and the terminal SiFA-COOH (**27**). SiFA-COOH (**27**) was produced by simple oxidation of SiFA-CHO (**12**) with potassium permanganate and served as labeling synthon instead of SiFA-CHO (**12**) in this case.[29] Mass spectrometric analysis of peptides **14**−**17** revealed unusual solvent adducts. Whereas the expected signals matching M + 2H$^+$ could be detected in the case of peptides **14** and **15**, very pronounced signals were observed for all RGD peptides matching the correct structure, but incremented by a constant value. Experiments with different deuterated solvents strongly indicate the formation of stable solvent adducts with MeCN and MeOH, although an unambiguous proof of adduct identity cannot be given at this point.

The labeling reaction is identical for PESIN and RGD peptides and occurs at the SiFA moiety via displacement of

dx.doi.org/10.1021/bc400588e | *Bioconjugate Chem.* 2014, 25, 738−749

Scheme 2. Synthesis of [^{18}F]SiFA-Labeled RGD Peptides

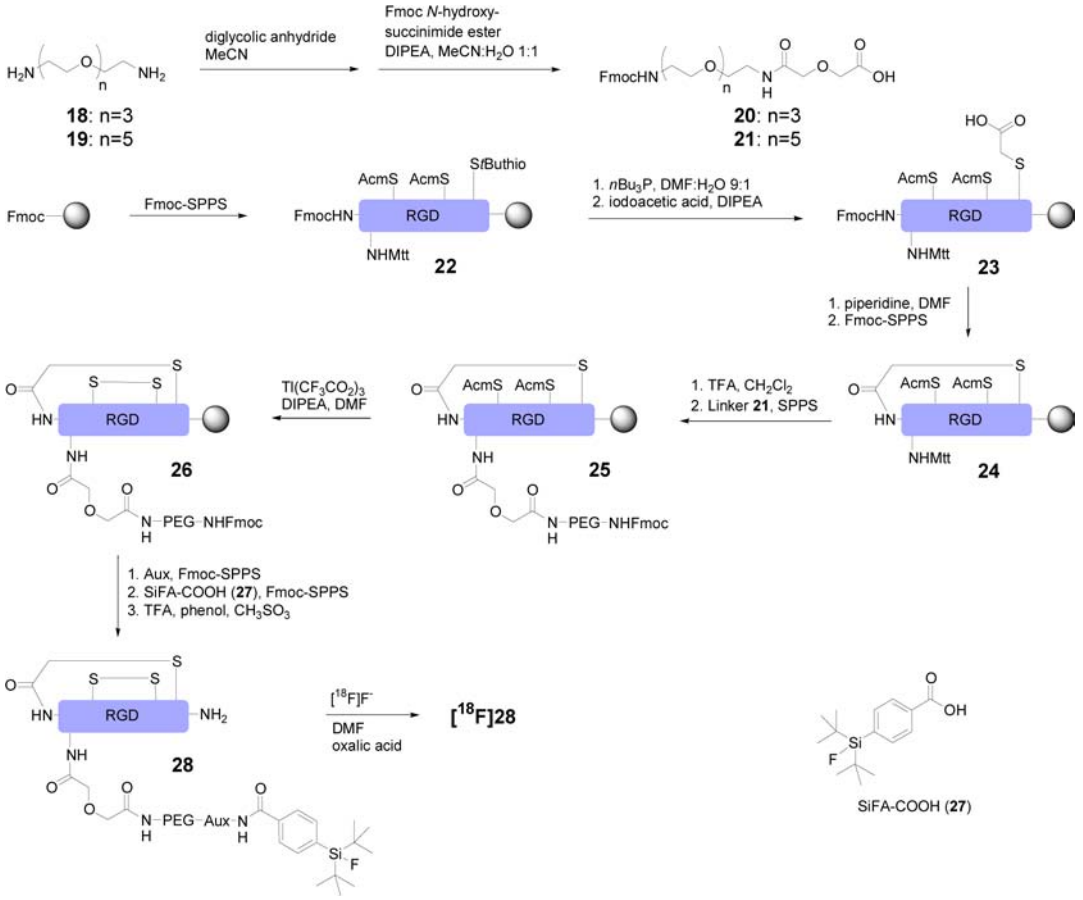

[^{19}F]fluoride by [^{18}F]fluoride. The preparation of reactive [^{18}F]fluoride was achieved by a cartridge based drying technique, the so-called Munich method.[30] In the presence of oxalic acid, a labeling efficiency of 75−95% was obtained within 15 min at ambient temperature. A simple C18 SPE cartridge purification yielded the desired peptides in 41−62% decay-corrected radiochemical yields and ≥99% radiochemical purity (Tables 1 and 2).

Stability Studies. All compounds were tested for stability in human plasma of healthy donors at 37 °C. No significant degradation was observed within 120 min for PESIN derivatives [^{18}F]**1**−[^{18}F]**9** and RGD peptides [^{18}F]**14** − [^{18}F]**17**.

Lipophilicity. LogD (1-octanol/phosphate buffer 0.05 M, pH = 7.4) values were determined as a measure of the overall lipophilicity of the compounds. Introduction of polar auxiliaries entailed a considerable decrease of lipophilicity for PESIN derivatives (Table 1) and RGD peptides (Table 2).

In Vitro Binding Affinity Determination Studies. Competitive displacement experiments were performed in vitro to evaluate the binding affinity of the modified compounds. PESIN derivatives were tested on PC3 cells for binding affinity toward the GRP receptor using ^{125}I-[Tyr^4]-Bombesin as the GRP receptor specific radioligand. IC_{50} values were determined to be between 7.0 ± 1.2 nM and 32 ± 1.1 nM (Table 1). RGD peptides were tested on U87MG cells for their affinity toward $\alpha_v\beta_3$ integrins. ^{125}I-Echistatin was applied as the $\alpha_v\beta_3$ specific radioligand. Only low affinities in the μM range were found on U87MG cells (Table 2).

In Vivo Biodistribution Studies. The assessment of the pharmacokinetic profile of the compounds was done by small animal PET imaging of tumor bearing mice. Male SCID mice with subcutaneous PC3 xenografts in the right flank were injected with approximately 10 MBq of the respective radiolabeled PESIN derivative and scanned dynamically over 120 min. A high tracer accumulation was observed immediately in the liver suggesting a mainly hepatobiliary clearance. In

Table 1. LogD, IC_{50} Values, and Yields of PESIN Derivatives [^{18}F]1−[^{18}F]9

entry	compound	logD[a]	IC_{50} [nM][a]	labeling yield [%][b]	isolated yield d.c. [%][b]
1	SiFA-PESIN (**1**)	2.29 ± 0.04	32 ± 1.1	86 ± 6	50 ± 5
2	SiFA-Asn(AcNH-β-Glc)-PESIN (**2**)	1.97 ± 0.04	7.5 ± 1.1	94 ± 3	54 ± 1
3	SiFA-Ser(β-Lac)-PESIN (**3**)	1.44 ± 0.01	32 ± 1.1	83 ± 2	54 ± 4
4	SiFA-Cya-PESIN (**4**)	1.41 ± 0.03	14 ± 1.2	92 ± 2	59 ± 3
5	SiFA-LysMe$_3$-PESIN (**5**)	0.48 ± 0.06	19 ± 1.1	90 ± 3	41 ± 2
6	SiFA-γ-carboxy-D-Glu-PESIN (**6**)	0.34 ± 0.02	10 ± 1.1	95 ± 1	56 ± 0
7	SiFA-Cya$_2$-PESIN (**7**)	−0.41 ± 0.04	7.0 ± 1.2	86 ± 0	59 ± 8
8	SiFA-LysMe$_3$-γ-carboxy-D-Glu-PESIN (**8**)	−0.71 ± 0.03	15 ± 1.1	93 ± 2	61 ± 0
9	SiFA-(γ-carboxy-D-Glu)$_2$-PESIN (**9**)	−1.22 ± 0.06	27 ± 1.1	91 ± 1	62 ± 1

[a]Mean ± SD (n = 3). [b]Mean ± SD (n = 2).

dx.doi.org/10.1021/bc400588e | Bioconjugate Chem. 2014, 25, 738−749

Table 2. LogD, IC_{50} Values, and Yields of RGD Derivatives [^{18}F]14–[^{18}F]17

entry	compound	logD[a]	IC_{50} [μM][a]	labeling yield [%][b]	isolated yield d.c. [%][b]
1	SiFA-RGD (**14**)	−1.10 ± 0.03	6.7 ± 1.1	77 ± 5	45 ± 3
2	SiFA-γ-carboxy-D-Glu-RGD (**15**)	−1.51 ± 0.03	6.5 ± 1.1	87 ± 4	57 ± 8
3	SiFA-(γ-carboxy-D-Glu)$_2$-RGD (**16**)	−1.85 ± 0.06	6.4 ± 1.0	75 ± 6	43 ± 4
4	SiFA-LysMe$_3$-γ-carboxy-D-Glu-RGD (**17**)	−1.97 ± 0.12	2.6 ± 1.1	82 ± 6	43 ± 6

[a]Mean ± SD (n = 3). [b]Mean ± SD (n = 2).

contrast, the tumor uptake was very poor and essentially remained on a constant low level. Since the tumor could hardly be distinguished from the background signal, no further experiments with PESIN analogues were performed.

RGD peptides were analyzed in the same manner using female SCID mice with subcutaneous U87MG xenografts in the right flank (Figure 3). The unmodified peptide [^{18}F]**14** showed

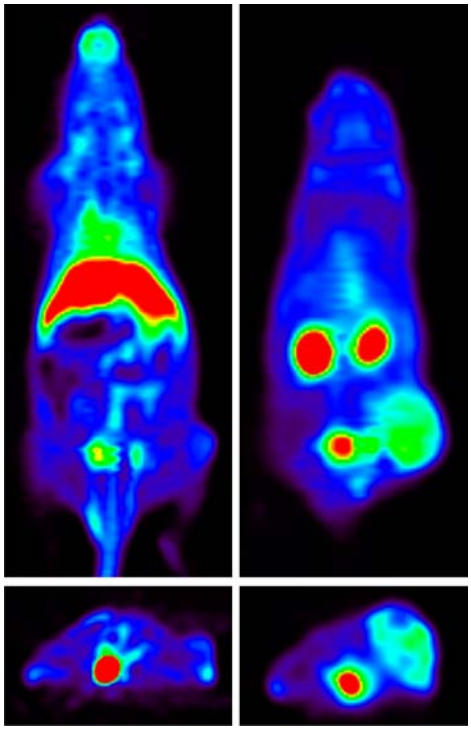

Figure 3. Coronal and transverse small animal PET images of mice bearing a U87MG xenograft in the right flank 120 min after injection of 10 MBq of ^{18}F-SiFA-RGD [^{18}F]**14** (left side) and ^{18}F-SiFA-LysMe$_3$-γ-carboxy-D-Glu-RGD [^{18}F]**17** (right side).

a similar behavior like the PESIN analogues and was characterized by a high tracer accumulation in the liver and only low uptake in the tumor, whereas a marked increase of [^{18}F]fluoride deposition was observed in the bones. This effect was not found in the case of the other RGD derivatives, and no simple explanation can be given for this observation as all derivatives comprise the same SiFA building block. The tumor to muscle ratio decreased over time from 2.54 ± 0.27 after 60 min to 1.64 ± 0.31 after 120 min. Peptides [^{18}F]**15** and [^{18}F]**16** showed a slightly increasing tumor to muscle ratio over time up to 3.53 ± 1.19 for [^{18}F]**15** and 3.99 ± 2.29 for [^{18}F]**16** after 120 min. The highest level of tumor to muscle ratio was observed with peptide [^{18}F]**17** which was determined to be 7.75 ± 1.66 after 120 min. Tracer accumulation in the liver played a minor role, whereas accumulation in the kidneys and bladder was predominant, which suggests a mainly renal elimination of the tracer. The accumulation of the tracer in the tumor was highest within the first 15 min followed by a constant but rapid wash-out. The $\alpha_v\beta_3$ specific tumor accumulation of RGD peptide [^{18}F]**17** was proven by coinjection of a 2000-fold excess of nonradioactive c(RGDyK). The tumor was clearly visible under baseline conditions, but visualization was exclusively and almost completely suppressed under blocking conditions (Figure 4).

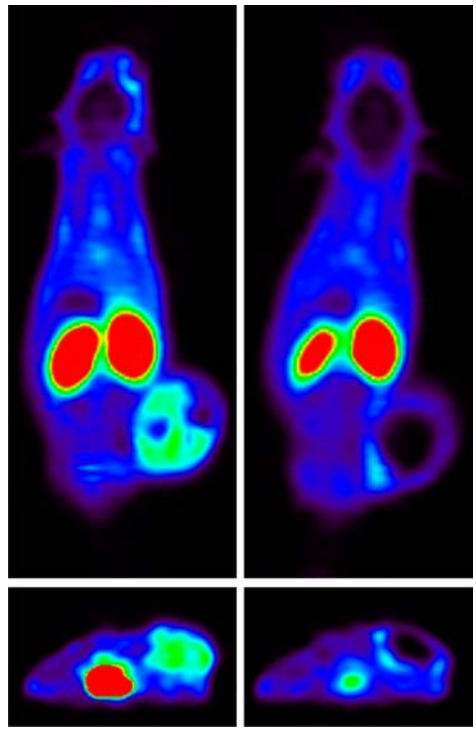

Figure 4. Coronal and transverse small animal PET images of mice bearing a U87MG xenograft in the right flank 120 min after injection of 10 MBq of ^{18}F-SiFA-LysMe$_3$-γ-carboxy-D-Glu-RGD [^{18}F]**17** under baseline (left side) and under blocking conditions (right side).

As the small animal PET data obtained for the RGD peptides were promising, biodistribution experiments were performed. The results obtained for the most promising RGD analogue [^{18}F]**17** are shown in Table 3. Tumor uptake was initially high with 5.30 ± 1.05% ID/g and decreased within 3 h to 0.66 ± 0.07% ID/g. Highest activity was observed in the kidneys, whereas liver, gallbladder, and intestine showed rather low activity levels suggesting predominantly renal excretion. Accumulation of activity in the bones was relatively high at early time points, but decreased steadily over time. In vivo metabolite studies revealed spontaneous formation of a more hydrophilic product already after 10 min p.i. in blood and urine samples (Figure 5). Further degradation of the tracer in blood was not observed. Analysis of urine samples showed a minor signal which might indicate the release of small amounts of [^{18}F]fluoride. The tracer is rapidly cleared from the blood (0.03% ID/g at 180 min p.i.) and from muscle (0.07 ± 0.01%

dx.doi.org/10.1021/bc400588e | Bioconjugate Chem. 2014, 25, 738−749

Table 3. Biodistribution of [^{18}F]17 in Nude Mice Bearing U87MG Xenografts at Different Times p.i.[a]

tissue	10 min	30 min	90 min	180 min
blood	5.31 ± 1.38	1.45 ± 0.37	0.14 ± 0.02	0.03 ± 0.00
heart	2.13 ± 0.49	0.66 ± 0.15	0.17 ± 0.03	0.09 ± 0.01
lung	3.25 ± 0.71	1.17 ± 0.20	0.37 ± 0.04	0.25 ± 0.04
liver	1.90 ± 0.27	0.92 ± 0.15	0.58 ± 0.08	0.43 ± 0.04
gallbladder	9.17 ± 3.95	1.57 ± 0.33	1.21 ± 0.24	3.20 ± 2.09
kidney	11.9 ± 3.69	5.85 ± 0.74	3.97 ± 0.57	3.01 ± 0.12
pancreas	1.05 ± 0.29	0.36 ± 0.06	0.18 ± 0.08	0.11 ± 0.02
spleen	1.31 ± 0.42	0.67 ± 0.17	0.44 ± 0.19	0.36 ± 0.09
stomach	1.93 ± 0.32	0.76 ± 0.10	0.50 ± 0.09	0.33 ± 0.08
intestine	1.73 ± 0.32	0.85 ± 0.16	0.59 ± 0.20	0.59 ± 0.13
muscle	1.44 ± 0.40	0.62 ± 0.38	0.15 ± 0.06	0.07 ± 0.01
bone	1.60 ± 0.25	0.96 ± 0.14	0.74 ± 0.10	0.53 ± 0.07
tumor	5.30 ± 1.05	2.30 ± 0.50	0.92 ± 0.10	0.66 ± 0.07
tumor/muscle	3.92 ± 1.25	4.55 ± 1.77	7.17 ± 2.95	9.67 ± 1.12
tumor/blood	1.04 ± 0.29	1.62 ± 0.26	6.81 ± 1.93	19.08 ± 2.42

[a]Results are expressed as % ID/g ± SD (n = 5).

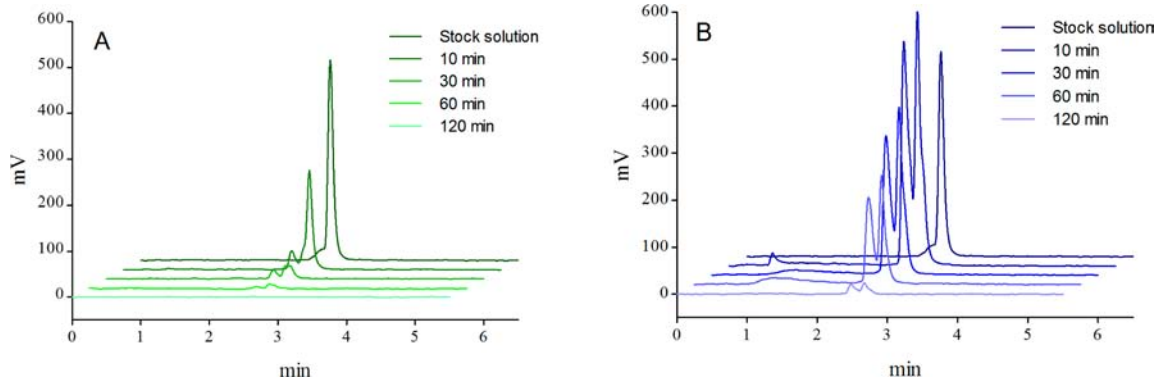

Figure 5. In vivo metabolism of ^{18}F-SiFA-LysMe$_3$-γ-carboxy-D-Glu-RGD [^{18}F]**17** in murine plasma (A) and urine (B).

ID/g at 180 min p.i.) which resulted in a favorable tumor-to-muscle ratio of 9.67 ± 1.12% ID/g and a high tumor-to-blood ratio of 19.08 ± 2.42% ID/g at 180 min p.i.

DISCUSSION

In order to adjust the pharmacokinetic properties of the peptide PESIN, several hydrophilic residues were introduced at the N-terminus where structural diversity is rather tolerated, as the N-terminal region has a lower impact on biological activity. Carbohydrates gave positive results in similar works and the influence of charge was also addressed previously.[31−33] To maintain the biological potency, no structural modifications were made at the pharmacophoric C-terminal binding site. The synthesis was straightforward and enabled the production of the peptides on solid support in good yields and high purities. The labeling synthon SiFA-CHO (**12**) was attached terminally which enables the incorporation of fluorine-18 (^{18}F) via nucleophilic displacement of [^{19}F]fluoride. Usually isotopic exchange comes along with low specific activities. However, very low precursor quantities of only 25 nmol were used, which abrogates this effect giving specific activities of up to 60 GBq μmol^{-1}. Recently, one of the major advances in the preparation of ^{18}F-labeled compounds was achieved with the cartridge based drying technique of [^{18}F]fluoride, the so-called Munich method.[30] An adapted protocol which was developed for the labeling of SiFA tagged peptides was applied.[34] Aqueous [^{18}F]fluoride was trapped on a strong anion exchange cartridge and released using a lyophilized mixture of [K⊂2.2.2]OH redissolved in DMF. It has to be considered that the stability of the Kryptofix complex in DMF is very limited. However, if applied directly after solubilizing, an elution efficiency of 95% of [K⊂2.2.2]^{18}F from the cartridge was achieved. The eluate was used directly for the labeling reaction. A precise amount of oxalic acid has to be added to partly neutralize the basic milieu, which is very important as it has a strong impact on the efficiency of the labeling reaction. Under these conditions the isotopic exchange proceeds without formation of byproducts, making a final HPLC separation of the radiolabeled peptides dispensable. From a chemical perspective, this method confers several advantages compared to methods in the literature which often suffer from lengthy and laborious multistep synthetic procedures. However, another powerful one-step ^{18}F-labeling approach using Al^{18}F-chelation emerged recently.[35,36] A comparison of the latest optimized procedures is given in Table 4.[37] Both approaches get along without azeotropic drying and HPLC purification shortening the overall synthesis time to 20 min. Most strikingly, SiFA labeling occurs at ambient temperature allowing the labeling of even sensitive biomolecules, whereas Al^{18}F labeling conditions are rather harsh. It is also noteworthy that the yields, purities, and specific activities achieved in this report are slightly higher.

Encouraged by the good binding affinities of the RGD peptide [^{18}F]-AH11185 to $\alpha_v\beta_3$ and $\alpha_v\beta_5$ integrins in vitro[28] and the promising clinical results, we decided to combine its

dx.doi.org/10.1021/bc400588e | Bioconjugate Chem. 2014, 25, 738−749

Table 4. Comparison of ^{18}F Labeling Approaches Using Al^{18}F Chelation[37] and SiFA Technology

parameter	Al^{18}F approach	SiFA approach
yield	42%	41−62%
purity	>95%	>99%
specific activity	37 GBq/μmol	60 GBq/μmol
synthesis time	20 min	20 min
temperature	100 °C	rt
azeotropic drying	not req.	not req.
purification	C18 SPE	C18 SPE

favorable properties with the advantages of the SiFA labeling technology. However, the reported synthesis[28] turned out to be inconvenient, as we intended to gain structural diversity by the introduction of different auxiliary amino acids into the peptide scaffold. Thus, we developed a new synthetic approach which enabled the entire synthesis of the peptide on solid support. A new protecting group strategy maintained full orthogonality. The direct attachment of SiFA-COOH (**27**) via SPPS proved to be superior over the coupling step with SiFA-CHO (**12**) in liquid phase, as it bypassed a troublesome purification of the aminooxyacetic acid functionalized peptide and reduced the overall synthesis steps at the same time. Radiolabeling of RGD and PESIN derivatives was carried out using the same experimental conditions.

Competitive displacement experiments revealed good affinities of the PESIN analogs toward the GRP receptor on PC3 cells showing that the introduction of a SiFA moiety at the N-terminus does not impede the biological function of the peptide, still maintaining a high affinity to the receptor in the nM range. However, small animal PET images showed an unfavorably high accumulation of the PESIN derivatives in the liver, although the lipophilicity of the compounds could be significantly reduced from 2.29 to −1.22. This result is in line with findings by Dijkgraaf et al. who found high uptake in the abdominal cavity with an Al^{18}F labeled bombesin derivative in spite of an even lower logD value of −1.47.[38] Nevertheless, the IC_{50} value was in the subnanomolar range and the tumor could be clearly visualized. In this report, the lipophilic character of the peptides seems to be too pronounced still and could not be compensated by high receptor affinities. Furthermore, PET images suggest that the tumors were potentially poorly vascularized or even necrotic which also impeded the effective visualization of the tumor.

High liver uptake was also obtained with the unmodified RGD peptide [^{18}F]**14** which is innately rather hydrophilic showing a logD value of −1.10. Accordingly, the tumor could be clearly visualized. Modification of the RGD sequence and concomitant decrease of logD values resulted in a further relevant improvement of the pharmacokinetic profile. The rather slow decrease of activity in bone of peptide [^{18}F]**17** may indicate that defluorination and subsequent deposition of [^{18}F]fluoride in the bones has taken place. However, in vivo metabolic stability studies did not show the presence of [^{18}F]fluoride in murine blood, and only low levels of [^{18}F]fluoride in urine were observed. Instead, tracer [^{18}F]**17** was to some extent converted into another more polar metabolite. Therefore, the relatively high bone uptake may be a result of several factors and is not necessarily a result of defluorination processes alone. Due to the fast clearance from the tissues, the obtained imaging results are rather inferior compared to other biological data reported in the literature. Tumor uptake of an Al^{18}F labeled cyclic RGD monomer, for example, was considerably higher,[39] even though concerns about patient safety due to the toxicity of aluminum metals in the central nervous system remain.[40,41] Thus, further refinements of SiFA-tagged RGD compounds will be the focus of further studies.

For the developed SiFA-derivatized RGD peptides, binding affinities on a μM level were rather poor and much higher than IC_{50} values reported in the literature where competition experiments were carried out on EA-Hy926 membrane fractions.[28] Nevertheless, the tumor uptake was clearly enhanced, which shows that the overall lipophilicity is more decisive for the in vivo behavior of the peptide derivative than the achieved binding affinities. Correlation of logD values and in vivo behavior indicates that logD values below −1.5 are needed to avoid unwanted hepatobiliary clearance. Peptide [^{18}F]**17** exhibited not only the best receptor affinity, but also the highest tumor uptake. It can be assumed that the additional positive charge might have a beneficial effect on these parameters. The blood clearance is exceptionally fast, 3-fold faster than in case of peptide [^{18}F]**16** over 180 min. All peptides are characterized by a rapid washout from all tissues. This can be explained by an enforced externalization of lipophilic compounds from the cell. A possible strategy to overcome this effect might be the multimerization of RGD peptides which was shown to be a powerful strategy to prevent this process as a consequence of increased avidities due to multivalency.[42]

CONCLUSION

Herein, we report the synthesis, radiolabeling, and biological evaluation of SiFA-tagged PESIN and RGD derivatives. Plasma stabilities, binding affinities, and logD values were determined for each peptide analogue. In the case of RGD peptides, it was demonstrated that the high lipophilicity of the SiFA synthon could be successfully compensated by the introduction of polar auxiliary amino acid residues into the peptide scaffold in favor of a better pharmacokinetic profile. Especially ^{18}F-SiFA-LysMe$_3$-γ-carboxy-D-Glu-RGD [^{18}F]**17** revealed a high tumor uptake and a rapid blood clearance in U87MG tumor bearing mice by means of small animal PET and biodistribution experiments.

EXPERIMENTAL SECTION

General. All reagents were purchased from commercial sources and were used without further purification. Solvents of at least p.a. quality were used. The resin for solid-phase peptide synthesis and amino acids was purchased from NovaBiochem and Bachem, coupling reagents from SigmaAldrich and Fluka. ^{125}I-[Tyr]^4-Bombesin and ^{125}I-Echistatin were obtained from PerkinElmer. Sep-Pak Accell Plus QMA carbonate light cartridges and Sep-Pak C18 light cartridges were obtained from Waters.

RPMI 1640 medium, fetal bovine serum, and L-glutamine were purchased from PAA; GlutaMax I medium was purchased from Gibco. Dulbecco's phosphate buffered saline (PBS) and bovine serum albumin were obtained from SigmaAldrich.

Analytical HPLC was done on an Agilent 1200 system using a Chromolith Performance (RP-18e, 100 × 4.6 mm, Merck, Germany) column. For preparative HPLC, a SymmetryPrep (C18, 19 × 300 mm, Waters, Germany) column was applied. ESI (Electrospray Ionization) MS spectra were measured on a

dx.doi.org/10.1021/bc400588e | Bioconjugate Chem. 2014, 25, 738−749

Finnigan MAT95Q instrument. Calculated values and corresponding found mass values are reported. The γ-counter used for radioactivity determination was a Packard Cobra Quantum. Small animal PET images were acquired using the Siemens Inveon P120 Dedicated PET system (Siemens Preclinical Imaging, Knoxville, TN, USA).

Peptide Synthesis. Solid-phase peptide synthesis for PESIN derivatives was carried out using the standard Fmoc strategy on an Fmoc-functionalized Rink Amide resin (loading: 0.74 mmol/g). A solution of the amino acid (4 equiv) and HBTU (*O*-(benzotriazol-1-yl)-*N*,*N*,*N*′,*N*′-tetramethyluronium hexafluorophosphate, 4 equiv) in DMF was treated with DIPEA (*N*,*N*-diisopropylethylamine, 4 equiv) for 2 min at ambient temperature, the mixture was then added to the resin bound unprotected peptide and shaken for 45 min at room temperature. Subsequently, the resin was washed with DMF (6×). The Fmoc protecting group was removed by washing the resin twice with 50% (v/v) piperidine in DMF (1 × 2 min, 1 × 5 min) and finally with DMF (6×). All steps were repeated until peptide elongation was complete. Finally, the resin was washed with CH_2Cl_2 (6×) and diethyl ether (3×) and dried in vacuo. The peptide was cleaved from the resin with TFA/H_2O/TIS (triisopropylsilane) 90:5:5 (1 mL) within 45 min at ambient temperature and precipitated in ice cold diethyl ether. The precipitate was separated by centrifugation, washed twice with diethyl ether, dried in vacuo, and finally purified by preparative HPLC (0−45% MeCN + 0.1% formic acid over 30 min). After lyophilization the peptide intermediate was dissolved in phosphate buffer (0.1 M, pH = 4, 400 μL) and mixed with SiFA-CHO (**12**) (1.1 equiv) in a volume of MeCN which is sufficient for complete dissolution of the aldehyde. After 5 min the product was purified by preparative HPLC (0−65% MeCN + 0.1% formic acid over 22 min) and lyophilized. All PESIN syntheses were typically performed in a 0.05−0.30 mmol scale according to this general procedure.

*Synthesis of SiFA-PESIN (**1**).* The elongation of the peptide chain was conducted with the following amino acids: Fmoc-Met-OH, Fmoc-Leu-OH, Fmoc-His(Trt)-OH, Fmoc-Gly-OH, Fmoc-Val-OH, Fmoc-Ala-OH, Fmoc-Trp(Boc)-OH, Fmoc-Gln(Trt)-OH, Fmoc-NH-PEG_4-COOH, and bis-Boc-aminooxyacetic acid (bis-Boc-Aoa). SiFA-PESIN was isolated as white solid (23%). ESI-MS: m/z (M + $2H^+$) calcd for $C_{71}H_{112}FN_{15}O_{16}SSi$: 1509.7875, found: 1509.7886.

*Synthesis of SiFA-Asn(AcNH-β-Glc)-PESIN (**2**).* The following amino acids were used: Fmoc-Met-OH, Fmoc-Leu-OH, Fmoc-His(Trt)-OH, Fmoc-Gly-OH, Fmoc-Val-OH, Fmoc-Ala-OH, Fmoc-Trp(Boc)-OH, Fmoc-Gln(Trt)-OH, Fmoc-NH-PEG_4-COOH, Fmoc-Asn(Ac_3AcNH-β-Glc)-OH, and bis-Boc-Aoa. After cleavage from the resin the peptide was dissolved in MeOH and treated with NaOMe (0.5 M in MeOH) until the pH of the mixture reached 12. The solution was shaken for 30 min at ambient temperature. After acidification with neat TFA the solvent was evaporated in a stream of nitrogen and the residual solid was coupled with SiFA-CHO (**12**) as described before. SiFA-Asn(AcNH-β-Glc)-PESIN was isolated as white solid (14%). ESI-MS: m/z (M + $2H^+$) calcd for $C_{83}H_{132}FN_{18}O_{23}SSi$: 1826.9109, found: 1826.9094.

*Synthesis of SiFA-Ser(β-Lac)-PESIN (**3**).* The following amino acids were used: Fmoc-Met-OH, Fmoc-Leu-OH, Fmoc-His(Trt)-OH, Fmoc-Gly-OH, Fmoc-Val-OH, Fmoc-Ala-OH, Fmoc-Trp(Boc)-OH, Fmoc-Gln(Trt)-OH, Fmoc-NH-PEG_4-COOH, Fmoc-Ser(Ac_7-β-Lac)-OH, and bis-Boc-Aoa. SiFA-Ser(β-Lac)-PESIN was isolated as white solid (10%). ESI-MS: m/z (M + $2H^+$) calcd for $C_{86}H_{137}FN_{16}O_{28}SSi$: 1920.9251, found: 1920.9264.

*Synthesis of SiFA-Cya-PESIN (**4**).* The following amino acids were used: Fmoc-Met-OH, Fmoc-Leu-OH, Fmoc-His(Trt)-OH, Fmoc-Gly-OH, Fmoc-Val-OH, Fmoc-Ala-OH, Fmoc-Trp(Boc)-OH, Fmoc-Gln(Trt)-OH, Fmoc-NH-PEG_4-COOH, Fmoc-Cya-OH, and bis-Boc-Aoa. Coupling of Fmoc-Cya-OH to the peptide was achieved with 8 equiv of DIPEA. SiFA-Cya-PESIN was isolated as white solid (6%). ESI-MS: m/z (M + $2H^+$) calcd for $C_{74}H_{117}FN_{16}O_{20}S_2Si$: 1660.7825, found: 1660.7840.

*Synthesis of SiFA-Cya$_2$-PESIN (**5**).* The following amino acids were used: Fmoc-Met-OH, Fmoc-Leu-OH, Fmoc-His(Trt)-OH, Fmoc-Gly-OH, Fmoc-Val-OH, Fmoc-Ala-OH, Fmoc-Trp(Boc)-OH, Fmoc-Gln(Trt)-OH, Fmoc-NH-PEG_4-COOH, Fmoc-Cya-OH, Fmoc-Cya-OH, and bis-Boc-Aoa. Coupling of Fmoc-Cya-OH to the peptide was achieved with 8 equiv of DIPEA. SiFA-Cya$_2$-PESIN was isolated as white solid (6%). ESI-MS: m/z (M + $2H^+$) calcd for $C_{77}H_{122}FN_{17}O_{24}S_3Si$: 1811.7764, found: 1811.7776.

*Synthesis of SiFA-LysMe$_3$-PESIN (**6**).* The following amino acids were used: Fmoc-Met-OH, Fmoc-Leu-OH, Fmoc-His(Trt)-OH, Fmoc-Gly-OH, Fmoc-Val-OH, Fmoc-Ala-OH, Fmoc-Trp(Boc)-OH, Fmoc-Gln(Trt)-OH, Fmoc-NH-PEG_4-COOH, Fmoc-LysMe$_3$-OH chloride, and bis-Boc-Aoa. SiFA-LysMe$_3$-PESIN was isolated as white solid (11%). ESI-MS: m/z (M + $2H^+$) calcd for $C_{80}H_{131}FN_{17}O_{17}SSi$: 1680.9383, found: 1680.9334.

*Synthesis of SiFA-γ-carboxy-D-Glu-PESIN (**7**).* The following amino acids were used: Fmoc-Met-OH, Fmoc-Leu-OH, Fmoc-His(Trt)-OH, Fmoc-Gly-OH, Fmoc-Val-OH, Fmoc-Ala-OH, Fmoc-Trp(Boc)-OH, Fmoc-Gln(Trt)-OH, Fmoc-NH-PEG_4-COOH, Fmoc-γ-carboxy-D-Glu(O*t*Bu)$_2$-OH, and bis-Boc-Aoa. SiFA-γ-carboxy-D-Glu-PESIN was isolated as white solid (25%). ESI-MS: m/z (M^{2-}) calcd for $C_{77}H_{115}FN_{16}O_{21}SSi$: 1678.7908, found: 1678.7914.

*Synthesis of SiFA-LysMe$_3$-γ-carboxy-D-Glu-PESIN (**8**).* The following amino acids were used: Fmoc-Met-OH, Fmoc-Leu-OH, Fmoc-His(Trt)-OH, Fmoc-Gly-OH, Fmoc-Val-OH, Fmoc-Ala-OH, Fmoc-Trp(Boc)-OH, Fmoc-Gln(Trt)-OH, Fmoc-NH-PEG_4-COOH, Fmoc-γ-carboxy-D-Glu(O*t*Bu)$_2$-OH, Fmoc-LysMe$_3$-OH chloride, and bis-Boc-Aoa. SiFA-LysMe$_3$-γ-carboxy-D-Glu-PESIN was isolated as white solid (10%). ESI-MS: m/z (M + H^+) calcd for $C_{86}H_{137}FN_{18}O_{22}SSi$: 1852.9618, found: 1852.9626.

*Synthesis of SiFA-(γ-carboxy-D-Glu)$_2$-PESIN (**9**).* The following amino acids were used: Fmoc-Met-OH, Fmoc-Leu-OH, Fmoc-His(Trt)-OH, Fmoc-Gly-OH, Fmoc-Val-OH, Fmoc-Ala-OH, Fmoc-Trp(Boc)-OH, Fmoc-Gln(Trt)-OH, Fmoc-NH-PEG_4-COOH, Fmoc-γ-carboxy-D-Glu(O*t*Bu)$_2$-OH, Fmoc-γ-carboxy-D-Glu(O*t*Bu)$_2$-OH, and bis-Boc-Aoa. SiFA-(γ-carboxy-D-Glu)$_2$-PESIN was isolated as white solid (17%). ESI-MS: m/z (M + $2H^+$ + Na^+) calcd for $C_{83}H_{125}FN_{17}O_{26}SSiNa$: 1877.8342, found: 1877.8362.

The solid-phase peptide synthesis of the RGD derivatives was carried out using the standard Fmoc strategy on a Fmoc-functionalized Rink Amide AM resin (loading: 0.79 mmol/g). A solution of the amino acid (4 equiv), HBTU (4 equiv), and HOBt (1-hydroxybenzotriazol, 4 equiv) in DMF was treated with DIPEA (4 equiv) for 2 min at ambient temperature; the mixture was then added to the resin bound unprotected peptide and shaken for 45 min at room temperature. Subsequently, the resin was washed with DMF (6×). The Fmoc protecting group

dx.doi.org/10.1021/bc400588e | *Bioconjugate Chem.* 2014, 25, 738−749

was removed by washing the resin twice with 50% (v/v) piperidine in DMF (1 × 2 min, 1 × 5 min) and finally with DMF (6×). All steps were repeated until peptide elongation was complete. The elongation of the peptide chain was done with following amino acids: Fmoc protected linker **20**, Fmoc-Cys(*t*Buthio)-OH, Fmoc-Phe-OH, Fmoc-Cys(Acm)-OH, Fmoc-Asp(O*t*Bu)-OH, Fmoc-Gly-OH, Fmoc-Arg(Pbf)-OH, Fmoc-Cys(Acm)-OH, and Fmoc-Lys(Mtt)-OH. The resin was then suspended in DMF:H_2O 9:1, treated with *n*-Bu_3P (50 equiv) under Ar-atmosphere twice for 60 min, and washed with DMF. Subsequently, the resin was mixed with iodoacetic acid (4 equiv) and DIPEA (1 equiv) in DMF and shaken for 45 min. Fmoc deprotection and coupling to the acetic acid according to standard SPPS conditions yielded the thioether. The solid supported cyclic peptide was washed with 1.75% TFA in CH_2Cl_2 at least 10 times until yellow color disappeared, washed successively with 10% DIPEA in CH_2Cl_2 and DMF, and coupled with Fmoc protected linker **21** under standard SPPS conditions. Treatment of the resin with $Tl(CF_3CO_2)_3$ (4 equiv) and DIPEA (2 equiv) in DMF for 45 min afforded the disulfide. The bicyclic peptide was deprotected with piperidine and coupled to another auxiliary amino acid and/or SiFA-COOH (**27**) using standard SPPS procedure. The peptide was finally cleaved from the resin with TFA (950 μL), phenol (25 mg), and CH_3SO_3 (25 μL) for 15 min at ambient temperature and precipitated in ice-cold diethyl ether. The precipitate was separated by centrifugation, washed twice with diethyl ether, and dried in vacuo. The product was purified by preparative HPLC (25−45% MeCN + 0.1% formic acid over 20 min) and lyophilized. All syntheses were typically done in a 0.1 mmol scale.

*Synthesis of Linker **20** and **21**.* A solution of diglycolic anhydride (1 equiv, 1 mmol) in 1 mL MeCN was added dropwise to a solution of polyethylene glycol bisamine (**18**, **19**) (1 equiv, 1 mmol) in 10 mL MeCN. The mixture was stirred at ambient temperature overnight. The solvent was removed in vacuo and the residue dissolved in MeCN:H_2O 1:1 (10 mL). DIPEA was added at 0 °C until pH reached 8 to 9 (approximately 0.5 mL), and a solution of Fmoc *N*-hydroxysuccinimide ester (1.3 equiv, 1.3 mmol) in 3 mL MeCN was added dropwise. After 1 h the mixture was warmed to room temperature and stirred overnight. After removal of the solvent, the product was purified by preparative HPLC (0−75% MeCN + 0.1% formic acid 0−30 min, 75−100% MeCN + 0.1% formic acid 30−30.5 min, 100% MeCN + 0.1% formic acid 30.5−35 min) and lyophilized (**20**: 47%, **21**: 40%).

*Linker **20**.* ^{1}H NMR (400 MHz, DMSO-d_6) δ (ppm) 12.85 (s, broad, 1H) 7.88 (d, J = 7.6 Hz, 2H), 7.83 (t, J = 5.6 Hz, 1H), 7.69 (d, J = 7.2 Hz, 2H), 7.40 (t, J = 7.6 Hz, 2H), 7.32 (m, 3H), 4.29 (d, J = 7.2 Hz, 2H), 4.20 (t, J = 6.4 Hz, 1H), 4.11 (s, 2H), 3.97 (s, 2H), 3.48 (s, 8H), 3.41 (m, 4H), 3.26 (q, J = 5.6 Hz, 2H), 3.13 (q, J = 6.0 Hz, 2H). ^{13}C NMR (100 MHz, DMSO-d_6) δ (ppm) 171.4, 168.8, 156.2, 143.9, 140.7, 127.6, 127.0, 125.2, 120.1, 70.0, 69.7, 69.5, 69.1, 68.8, 67.7, 65.3, 46.7, 40.1, 38.0. ESI-MS: m/z (M + Na^+) calcd for $C_{27}H_{34}N_2O_9Na$: 553.2157, found: 553.2155.

*Linker **21**.* ^{1}H NMR (400 MHz, DMSO-d_6) δ (ppm) 12.85 (s, broad, 1H), 7.88 (d, J = 7.6 Hz, 2H), 7.83 (t, J = 5.6 Hz, 1H), 7.69 (d, J = 7.6 Hz, 2H), 7.40 (t, J = 7.6 Hz, 2H), 7.33 (m, 3H), 4.29 (d, J = 7.2 Hz, 2H), 4.20 (t, J = 6.4 Hz, 1H), 4.11 (s, 2H), 3.96 (s, 2H), 3.48 (m, 16H), 3.41 (m, 4H), 3.26 (q, J = 5.6 Hz, 2H), 3.13 (q, J = 6.0 Hz, 2H). ^{13}C NMR (100 MHz, DMSO-d_6) δ (ppm) 172.0, 169.4, 156.7, 144.5, 141.3, 128.2, 127.6, 125.7, 120.7, 70.6, 70.3, 70.3, 70.3, 70.2, 70.1, 70.1, 69.6, 69.4, 68.3, 65.9, 47.3, 40.7, 38.6. ESI-MS: m/z (M + Na^+) calcd for $C_{31}H_{42}N_2O_{11}Na$: 641.2681, found: 641.2679.

*Synthesis of SiFA-RGD (**14**).* No auxiliary amino acid was used. SiFA-RGD was obtained as white solid (18%). ESI-MS: m/z (M + $2H^+$) calcd for $C_{81}H_{132}FN_{17}O_{26}S_3Si$: 1901.8434, found: 1901.9114.

*Synthesis of SiFA-γ-carboxy-D-Glu-RGD (**15**).* Fmoc-γ-carboxy-D-Glu-OH was introduced as auxiliary amino acid. SiFA-γ-carboxy-D-Glu-RGD was obtained as white solid (15%). ESI-MS: m/z (M + $2H^+$) calcd for $C_{87}H_{139}FN_{18}O_{31}S_3Si$: 2074.8758, found: 2074.9444.

*Synthesis of SiFA-(γ-carboxy-D-Glu)$_2$-RGD (**16**).* Two Fmoc-γ-carboxy-D-Glu-OH residues were subsequently introduced. SiFA-(γ-carboxy-D-Glu)$_2$-RGD was obtained as white solid (10%). ESI-MS: m/z (M + K^+ + H^+ + 2MeCN + 2MeOH) calcd for $C_{99}H_{159}FKN_{21}O_{38}S_3Si$: 2431.9696, found: 2432.0840.

*Synthesis of SiFA-LysMe$_3$-γ-carboxy-D-Glu-RGD (**17**).* Fmoc-LysMe$_3$-OH and Fmoc-γ-carboxy-D-Glu-OH residues were subsequently introduced. SiFA-LysMe$_3$-γ-carboxy-D-Glu-RGD was obtained as white solid (11%). ESI-MS: m/z (M^+ + K^+ + 2MeCN + 2 MeOH) calcd for $C_{102}H_{170}FKN_{22}O_{34}S_3Si$: 2429.0791, found: 2429.1970.

Radiolabeling. Aqueous [^{18}F]fluoride was produced via the $^{18}O(p,n)^{18}F$ nuclear reaction by irradiation of enriched [^{18}O]water. [^{18}F]Fluoride was loaded onto a SAX cartridge (Sep-Pak Accell Plus QMA Carbonate light, 46 mg). Twenty milliliters of air passed through the cartridge followed by 5 mL of anhydrous MeCN and a further 20 mL of air. [^{18}F]Fluoride was eluted from the cartridge with 0.5 mL of $[K^+\subset 2.2.2]OH^-$ (100 μmol) in anhydrous DMF. $[K^+\subset 2.2.2]OH^-$ was previously prepared from Kryptofix 2.2.2 (41 mg, 110 μmol) and 100 μL aqueous KOH (1 M, 100 μmol) and lyophilization of the Kryptofix solution to dryness. Subsequently, 37.5 μL oxalic acid in anhydrous DMF (0.5 M, 18.75 μmol) and 5 μL labeling precursor in anhydrous DMF (5 mM, 25 nmol) were added to the eluate. The labeling reaction was complete after 15 min at ambient temperature without stirring and an aliquot was taken for reaction control and analyzed by analytical HPLC. The mixture was diluted with 10 mL HEPES buffer (0.1 M, pH = 4) and passed through a Sep-Pak C18 light cartridge. The cartridge was rinsed with 5 mL of water to remove solvent residues. The purified product was eluted with 0.5 mL EtOH and diluted with isotonic saline solution (4.5 mL). The syntheses revealed radiochemical yields ranging from 41% to 62% after a synthesis time of 20 min and specific activities of up to 60 GBq μmol^{-1}. The radiochemical purities were ≥99%.

Lipophilicity. Five microliters of the purified [^{18}F]fluoride labeled peptide in ethanol were added to 400 μL 1-octanol and 400 μL phosphate buffer (0.05 M, pH = 7.4) and the mixture was vigorously vortexed for 5 min. After centrifugation at 14000 rpm for 1 min aliquots (300 μL) of both layers were collected and measured for radioactivity. The logD value was calculated as the log ratio of the radioactivity in the organic and aqueous layer.

Plasma Stability. 200 μL of an injectable solution of the radiolabeled peptide were mixed with 500 μL human plasma. The samples were incubated at 37 °C. At 10, 30, 60, and 120 min, aliquots were taken and analyzed by analytical HPLC.

Cell Culture. PC-3 prostate adenocarcinoma cells were grown in RPMI 1640 medium, human U87MG glioblastoma cells in DMEM, each supplemented with 10% (v/v) fetal

dx.doi.org/10.1021/bc400588e | *Bioconjugate Chem.* 2014, 25, 738−749

bovine serum and 1% (v/v) L-glutamine at 37 °C in a humidified CO_2 (5%) atmosphere.

Cell Binding Assay. In vitro binding affinities were measured via competitive displacement experiments using a Millipore Multiscreen punch kit. Millipore 96-well filter plates were incubated with 200 μL/well Dulbecco's phosphate buffered saline (PBS, modified, without $CaCl_2$ and $MgCl_2$, liquid, sterile-filtered, supplemented with 1 g/100 mL bovine serum albumin) for 1 h before use. PC-3 cells were harvested, suspended in Opti-MEM I (reduced serum medium, GlutaMax I), and seeded in 96-well plates at 10^5 cells per well. Subsequently, the cells were incubated on a shaker for 1 h at ambient temperature with 0.1 nM ^{125}I-[Tyr^4]-Bombesin (81.4 GBq/μmol) as the GRPR-specific radioligand in the presence of increasing concentrations (0−1 μM) of competing PESIN derivatives in a total volume of 100 μL. After incubation the cell pellets were washed 3 times (2 × 100 μL and 1 × 200 μL) with Dulbecco's phosphate buffered saline (PBS, modified, without $CaCl_2$ and $MgCl_2$, liquid, sterile-filtered) using the Millipore Multiscreen vacuum manifold for filtration. The filters were collected and measured for radioactivity in a γ-counter. Experiments were done at least three times in triplicate. The 50% inhibitory concentration (IC_{50}) value was calculated by nonlinear regression analysis using the GraphPad Prism Software program (v 5.03).

In vitro binding affinities of RGD peptides were measured analogously to the PESIN derivatives. U87MG cells were suspended in binding buffer (Tris·HCl 25 mM, NaCl 150 mM, $CaCl_2$ 1 mM, $MgCl_2$ 0.5 mM, $MnCl_2$ 1 mM, pH 7.4, BSA 0.1%) and incubated with 0.1 nM ^{125}I-Echistatin (81.4 GBq/μmol) as the $\alpha_v\beta_3$ specific radioligand in the presence of increasing concentrations (0−250 μM) of competing RGD peptides.

Animal Study. All animal experiments were performed in compliance with the current German animal protecting laws and protocols of the local authorities.

PET. Nude mice (SCID, male for PESIN derivatives, female for RGD peptides, 25−30 g, 2 animals per peptide) were injected with PC-3 or U87MG cells (5 × 10^6 cells/mouse) subcutaneously into the right flank. After tumor inoculation cells were allowed to grow for 6 to 8 weeks. Approximately 10 MBq of the PESIN or RGD tracer were injected via the tail vein under isoflurane anesthesia. Dynamic small animal PET images were acquired over 120 min. Data were divided into time frames from 10 s to 10 min for the assessment of temporal changes in regional tracer accumulation. The images were reconstructed using an OSEM3D/MAP algorithm. Regions of interest (ROIs) were defined for the quantification of tracer accumulation in different tissues.

Biodistribution. Nude mice (female SCID, 25−30 g, 20 animals per peptide) were injected with U87MG cells (5 × 10^6 cells/mouse) subcutaneously into the right flank. After tumor inoculation cells were allowed to grow for 6 to 8 weeks. Approximately 1−5 MBq of the RGD tracer were injected via the tail vein under isoflurane anesthesia. The animals were sacrificed after different time points (10, 30, 90, and 180 min, 5 animals for each time point) and the organs of interest were dissected and weighted. Radioactivity in the tissues was determined with a γ-counter. Data are given as % injected dose per g tissue.

In Vivo Stability Study. Nude mice (female SCID, 25−30 g, 1 animal per time point) were injected with approximately 150 MBq of ^{18}F-SiFA-LysMe$_3$-γ-carboxy-D-Glu-RGD [^{18}F]**17** via the tail vein under isoflurane anesthesia. Animals were sacrificed at 10, 30, 60, and 120 min after injection, and blood and urine were collected. Blood samples were centrifuged at 2500*g*, and the supernatants and urine samples were analyzed by analytical radio-HPLC.

■ ASSOCIATED CONTENT

Supporting Information

Data from analytical HPLC, binding curves, small animal PET images, and data from biodistribution experiments. This material is available free of charge via the Internet at http://pubs.acs.org/.

■ AUTHOR INFORMATION

Corresponding Authors

*Phone +49 (0)89 7095 69941, fax +49 (0)89 7095 7646, e-mail Simon.Lindner@med.uni-muenchen.de.

*Phone +49 (0)621 383 5594, fax +49 (0)621 383 1910, e-mail bjoern.waengler@medma.uni-heidelberg.de.

Notes

The authors declare no competing financial interest.

■ ACKNOWLEDGMENTS

We thank Dr. Werner Spahl for his help with ESI-MS, Dr. Lars Allmendinger for NMR measurements, and the members of the laboratory for preclinical imaging for their support with animal studies. We gratefully acknowledge financial support by the BMBF (German Federal Ministry of Education and Research) Leading Edge Cluster "m^4 − Personalized Medicine and Targeted Therapies".

■ REFERENCES

(1) Wängler, C., Kostikov, A., Zhu, J., Chin, J., Wängler, B., and Schirrmacher, R. (2012) Silicon-[^{18}F]fluorine radiochemistry: basics, applications and challenges. *Appl. Sci. 2*, 277−302.

(2) Schirrmacher, E., Wängler, B., Cypryk, M., Bradtmöller, G., Schäfer, M., Eisenhut, M., Jurkschat, K., and Schirrmacher, R. (2007) Synthesis of *p*-(Di-*tert*-butyl[^{18}F]fluorosilyl)benzaldehyde ([^{18}F]SiFA-A) with high specific activity by isotopic exchange: a convenient labeling synthon for the ^{18}F-labeling of N-amino-oxy derivatized peptides. *Bioconjugate Chem. 18*, 2085−2089.

(3) Höhne, A., Mu, L., Honer, M., Schubiger, P. A., Ametamey, S. M., Graham, K., Stellfeld, T., Borkowski, S., Berndorff, D., Klar, U., Voigtmann, U., Cyr, J. E., Friebe, M., Dinkelborg, L., and Srinivasan, A. (2008) Synthesis, ^{18}F-Labeling, and *in vitro* and *in vivo* studies of bombesin peptides modified with silicon-based building blocks. *Bioconjugate Chem. 19*, 1871−1879.

(4) Kostikov, A. P., Iovkova, L., Chin, J., Schirrmacher, E., Wängler, B., Wängler, C., Jurkschat, K., Cosa, G., and Schirrmacher, R. (2011) N-(4-(di-tert-butyl[^{18}F]fluorosilyl)benzyl)-2-hydroxy-N,N-dimethylethylammonium bromide ([^{18}F]SiFAN$^+$Br$^-$): A novel lead compound for the development of hydrophilic SiFA-based prosthetic groups for ^{18}F-labeling. *J. Fluorine Chem. 132*, 27−34.

(5) Dialer, L. O., Selivanova, S. V., Müller, C. J., Müller, A., Stellfeld, T., Graham, K., Dinkelborg, L. M., Krämer, S. D., Schibli, R., Reiher, M., and Ametamey, S. M. (2013) Studies toward the development of new silicon-containing building blocks for the direct 18F-labeling of peptides. *J. Med. Chem. 56*, 7552−7563.

(6) Cornelio, D., Roesler, R., and Schwartsmann, G. (2007) Gastrin-releasing peptide receptor as a molecular target in experimental anticancer therapy. *Ann. Oncol. 18*, 1457−1466.

(7) Reubi, J. C., Wenger, S., Schmuckli-Maurer, J., Schaer, J.-C., and Gugger, M. (2002) Bombesin receptor subtypes in human cancers: detection with the universal radioligand ^{125}I-[D-TYR^6, β-ALA^{11}, PHE^{13}, NLE^{14}] Bombesin(6−14). *Clin. Cancer Res. 8*, 1139−1146.

(8) Fani, M., and Maecke, H. R. (2012) Radiopharmaceutical development of radiolabelled peptides. *Eur. J. Nucl. Med. Mol. Imaging 39*, 11−30.
(9) Ananias, H. J. K., de Jong, I. J., Dierckx, R. A., de Wiele, C. v., Helfrich, W., and Elsinga, P. H. (2008) Nuclear imaging of prostate cancer with gastrin-releasing-peptide-receptor targeted radiopharmaceuticals. *Curr. Pharm. Des. 14*, 3033−3047.
(10) Abiraj, K., Jaccard, H., Kretzschmar, M., Helm, L., and Maecke, H. R. (2008) Novel DOTA-based prochelator for divalent peptide vectorization: synthesis of dimeric bombesin analogues for multimodality tumor imaging and therapy. *Chem. Commun.*, 3248−3250.
(11) Lane, S. R., Nanda, P., Rold, T. L., Sieckman, G. L., Figueroa, S. D., Hoffman, T. J., Jurisson, S. S., and Smith, C. J. (2010) Optimization, biological evaluation and microPET imaging of copper-64-labeled bombesin agonists, [^{64}Cu-NO2A-(X)-BBN(7−14)NH_2], in a prostate tumor xenografted mouse model. *Nucl. Med. Biol. 37*, 751−761.
(12) Schroeder, R. J., Müller, C., Reneman, S., Melis, M., Breeman, W. P., Blois, E., Bangma, C., Krenning, E., Weerden, W., and Jong, M. (2010) A standardised study to compare prostate cancer targeting efficacy of five radiolabelled bombesin analogues. *Eur. J. Nucl. Med. Mol. Imaging 37*, 1386−1396.
(13) Fournier, P., Dumulon-Perreault, V., Ait-Mohand, S., Langlois, R., Bénard, F., Lecomte, R., and Guérin, B. (2012) Comparative study of ^{64}Cu/NOTA-[D-Tyr^6,βAla^{11},Thi^{13},Nle^{14}]BBN(6−14) monomer and dimers for prostate cancer PET imaging. *Eur. J. Nucl. Med. Mol. Imaging Res. 2*, 1−15.
(14) Fournier, P., Dumulon-Perreault, V., Ait-Mohand, S., Tremblay, S., Bénard, F., Lecomte, R., and Guérin, B. (2012) Novel radiolabeled peptides for breast and prostate tumor PET imaging: ^{64}Cu/and ^{68}Ga/NOTA-PEG-[D-Tyr^6,βAla^{11},Thi^{13},Nle^{14}]BBN(6−14). *Bioconjugate Chem. 23*, 1687−1693.
(15) Nanda, P. K., Pandey, U., Bottenus, B. N., Rold, T. L., Sieckman, G. L., Szczodroski, A. F., Hoffman, T. J., and Smith, C. J. (2012) Bombesin analogues for gastrin-releasing peptide receptor imaging. *Nucl. Med. Biol. 39*, 461−471.
(16) Yu, Z., Carlucci, G., Ananias, H. K., Dierckx, R. J. O., Liu, S., Helfrich, W., Wang, F., de Jong, I., and Elsinga, P. (2013) Evaluation of a technetium-99m labeled bombesin homodimer for GRPR imaging in prostate cancer. *Amino Acids 44*, 543−553.
(17) Zhang, H., Schuhmacher, J., Waser, B., Wild, D., Eisenhut, M., Reubi, J., and Maecke, H. (2007) DOTA-PESIN, a DOTA-conjugated bombesin derivative designed for the imaging and targeted radionuclide treatment of bombesin receptor-positive tumours. *Eur. J. Nucl. Med. Mol. Imaging 34*, 1198−1208.
(18) Wild, D., Frischknecht, M., Zhang, H., Morgenstern, A., Bruchertseifer, F., Boisclair, J., Provencher-Bolliger, A., Reubi, J.-C., and Maecke, H. R. (2011) Alpha- versus beta-particle radiopeptide therapy in a human prostate cancer model (^{213}Bi-DOTA-PESIN and ^{213}Bi-AMBA versus^{177}Lu-DOTA-PESIN). *Cancer Res. 71*, 1009−1018.
(19) Cai, H., and Conti, P. S. (2013) RGD-based PET tracers for imaging receptor integrin $\alpha_v\beta_3$ expression. *J. Labelled Compd. Radiopharm. 56*, 264−279.
(20) Gaertner, F. C., Kessler, H., Wester, H. J., Schwaiger, M., and Beer, A. J. (2012) Radiolabelled RGD peptides for imaging and therapy. *Eur. J. Nucl. Med. Mol. Imaging 39*, 126−138.
(21) Tomasi, G., Kenny, L., Mauri, F., Turkheimer, F., and Aboagye, E. (2011) Quantification of receptor-ligand binding with [^{18}F]-fluciclatide in metastatic breast cancer patients. *Eur. J. Nucl. Med. Mol. Imaging 38*, 2186−2197.
(22) Battle, M. R., Goggi, J. L., Allen, L., Barnett, J., and Morrison, M. S. (2011) Monitoring tumor response to antiangiogenic sunitinib therapy with ^{18}F-fluciclatide, an ^{18}F-labeled $\alpha_V\beta_3$-integrin and $\alpha_v\beta_5$-integrin imaging agent. *J. Nucl. Med. 52*, 424−430.
(23) Beer, A. J., and Schwaiger, M. (2011) PET of $\alpha_v\beta_3$-integrin and $\alpha_v\beta_5$-integrin expression with ^{18}F-fluciclatide for assessment of response to targeted therapy: ready for prime time? *J. Nucl. Med. 52*, 335−337.
(24) Morrison, M. S., Ricketts, S.-A., Barnett, J., Cuthbertson, A., Tessier, J., and Wedge, S. R. (2009) Use of a novel Arg-Gly-Asp radioligand, ^{18}F-AH111585, to determine changes in tumor vascularity after antitumor therapy. *J. Nucl. Med. 50*, 116−122.
(25) McParland, B. J., Miller, M. P., Spinks, T. J., Kenny, L. M., Osman, S., Khela, M. K., Aboagye, E., Coombes, R. C., Hui, A.-M., and Cohen, P. S. (2008) The biodistribution and radiation dosimetry of the Arg-Gly-Asp peptide ^{18}F-AH111585 in healthy volunteers. *J. Nucl. Med. 49*, 1664−1667.
(26) Kenny, L. M., Coombes, R. C., Oulie, I., Contractor, K. B., Miller, M., Spinks, T. J., McParland, B., Cohen, P. S., Hui, A.-M., Palmieri, C., Osman, S., Glaser, M., Turton, D., Al-Nahhas, A., and Aboagye, E. O. (2008) Phase I trial of the positron-emitting Arg-Gly-Asp (RGD) peptide radioligand ^{18}F-AH111585 in breast cancer patients. *J. Nucl. Med. 49*, 879−886.
(27) Glaser, M., Morrison, M., Solbakken, M., Arukwe, J., Karlsen, H., Wiggen, U., Champion, S., Kindberg, G. M., and Cuthbertson, A. (2008) Radiosynthesis and biodistribution of cyclic RGD peptides conjugated with novel [^{18}F]fluorinated aldehyde-containing prosthetic groups. *Bioconjugate Chem. 19*, 951−957.
(28) Indrevoll, B., Kindberg, G. M., Solbakken, M., Bjurgert, E., Johansen, J. H., Karlsen, H., Mendizabal, M., and Cuthbertson, A. (2006) NC-100717: A versatile RGD peptide scaffold for angiogenesis imaging. *Bioorg. Med. Chem. Lett. 16*, 6190−6193.
(29) Iovkova, L., Wängler, B., Schirrmacher, E., Schirrmacher, R., Quandt, G., Boening, G., Schürmann, M., and Jurkschat, K. (2009) *para*-Functionalized aryl-di-*tert*-butylfluorosilanes as potential labeling synthons for ^{18}F radiopharmaceuticals. *Chem.—Eur. J. 15*, 2140−2147.
(30) Wessmann, S. H., Henriksen, G., and Wester, H.-J. (2012) Cryptate mediated nudeophilic ^{18}F-fluorination without azeotropic drying. *Nuklearmedizin 51*, 1−8.
(31) Wängler, C., Waser, B., Alke, A., Iovkova, L., Buchholz, H.-G., Niedermoser, S., Jurkschat, K., Fottner, C., Bartenstein, P., Schirrmacher, R., Reubi, J.-C., Wester, H.-J., and Wängler, B. (2010) One-step ^{18}F-labeling of carbohydrate-conjugated octreotate-derivatives containing a silicon-fluoride-acceptor (SiFA): in vitro and in vivo evaluation as tumor imaging agents for positron emission tomography (PET). *Bioconjugate Chem. 21*, 2289−2296.
(32) Mu, L., Honer, M., Becaud, J., Martic, M., Schubiger, P. A., Ametamey, S. M., Stellfeld, T., Graham, K., Borkowski, S., Lehmann, L., Dinkelborg, L., and Srinivasan, A. (2010) *In vitro* and *in vivo* characterization of novel ^{18}F-labeled bombesin analogues for targeting GRPR-positive tumors. *Bioconjugate Chem. 21*, 1864−1871.
(33) Honer, M., Mu, L., Stellfeld, T., Graham, K., Martic, M., Fischer, C. R., Lehmann, L., Schubiger, P. A., Ametamey, S. M., Dinkelborg, L., Srinivasan, A., and Borkowski, S. (2011) ^{18}F-labeled bombesin analog for specific and effective targeting of prostate tumors expressing gastrin-releasing peptide receptors. *J. Nucl. Med. 52*, 270−278.
(34) Wängler, C., Niedermoser, S., Chin, J., Orchowski, K., Schirrmacher, E., Jurkschat, K., Iovkova-Berends, L., Kostikov, A. P., Schirrmacher, R., and Wängler, B. (2012) One-step ^{18}F-labeling of peptides for positron emission tomography imaging using the SiFA methodology. *Nat. Protoc. 7*, 1946−1955.
(35) McBride, W. J., D'Souza, C. A., Sharkey, R. M., Karacay, H., Rossi, E. A., Chang, C.-H., and Goldenberg, D. M. (2010) Improved ^{18}F labeling of peptides with a fluoride-aluminum-chelate complex. *Bioconjugate Chem. 21*, 1331−1340.
(36) McBride, W. J., Sharkey, R. M., Karacay, H., D'Souza, C. A., Rossi, E. A., Laverman, P., Chang, C.-H., Boerman, O. C., and Goldenberg, D. M. (2009) A novel method of ^{18}F radiolabeling for PET. *J. Nucl. Med. 50*, 991−998.
(37) Wan, W., Guo, N., Pan, D., Yu, C., Weng, Y., Luo, S., Ding, H., Xu, Y., Wang, L., Lang, L., Xie, Q., Yang, M., and Chen, X. (2013) First experience of ^{18}F-alfatide in lung cancer patients using a new lyophilized kit for rapid radiofluorination. *J. Nucl. Med. 54*, 691−698.
(38) Dijkgraaf, I., Franssen, G. M., McBride, W. J., D'Souza, C. A., Laverman, P., Smith, C. J., Goldenberg, D. M., Oyen, W. J., and Boerman, O. C. (2012) PET of tumors expressing gastrin-releasing

peptide receptor with an ^{18}F-labeled bombesin analog. *J. Nucl. Med. 53*, 947−952.
(39) Shetty, D., Jeong, J. M., Kim, Y. J., Lee, J. Y., Hoigebazar, L., Lee, Y.-S., Lee, D. S., and Chung, J.-K. (2012) Development of a bifunctional chelating agent containing isothiocyanate residue for one step F-18 labeling of peptides and application for RGD labeling. *Bioorg. Med. Chem. 20*, 5941−5947.
(40) Shaw, C. A., and Tomljenovic, L. (2013) Aluminum in the central nervous system (CNS): toxicity in humans and animals, vaccine adjuvants, and autoimmunity. *Immunol. Res. 56*, 304−316.
(41) Li, L. (2003) The biochemistry and physiology of metallic fluoride: action, mechanism, and implications. *Crit. Rev. Oral Biol. Med. 14*, 100−114.
(42) Schottelius, M., Laufer, B., Kessler, H., and Wester, H.-J. (2009) Ligands for mapping $\alpha_v\beta_3$-integrin expression in vivo. *Acc. Chem. Res. 42*, 969−980.